JACS
JOURNAL OF THE AMERICAN CHEMICAL SOCIETY

Subscriber access provided by ISTANBUL TEKNIK UNIV

Communication

A One-Step Homogeneous Immunoassay for Cancer Biomarker Detection Using Gold Nanoparticle Probes Coupled with Dynamic Light Scattering

Xiong Liu, Qiu Dai, Lauren Austin, Janelle Coutts, Genevieve Knowles, Jianhua Zou, Hui Chen, and Qun Huo

J. Am. Chem. Soc., **2008**, 130 (9), 2780-2782 • DOI: 10.1021/ja711298b

Downloaded from http://pubs.acs.org on February 8, 2009

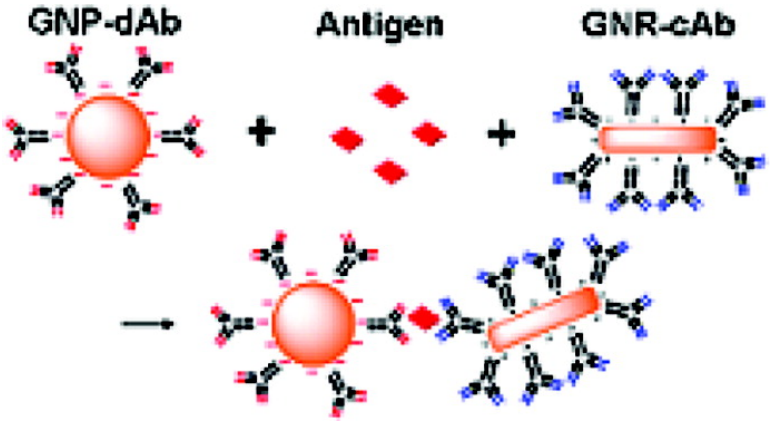

More About This Article

Additional resources and features associated with this article are available within the HTML version:

- Supporting Information
- Links to the 5 articles that cite this article, as of the time of this article download
- Access to high resolution figures
- Links to articles and content related to this article
- Copyright permission to reproduce figures and/or text from this article

View the Full Text HTML

ACS Publications
High quality. High impact.

Journal of the American Chemical Society is published by the American Chemical Society. 1155 Sixteenth Street N.W., Washington, DC 20036

J|A|C|S
COMMUNICATIONS

Published on Web 02/08/2008

A One-Step Homogeneous Immunoassay for Cancer Biomarker Detection Using Gold Nanoparticle Probes Coupled with Dynamic Light Scattering

Xiong Liu, Qiu Dai, Lauren Austin, Janelle Coutts, Genevieve Knowles, Jianhua Zou, Hui Chen, and Qun Huo*

Nanoscience Technology Center, Department of Chemistry, Department of Mechanical, Materials and Aerospace Engineering, University of Central Florida, 12424 Research Parkway Suite 400, Orlando, Florida 32826

Received December 20, 2007; E-mail: qhuo@mail.ucf.edu

Highly sensitive detection and accurate analysis of biomarker molecules in human fluid samples are essential for early detection, treatment and management of cancer. For a typical sandwich-type immunoassay which is routinely used for protein biomarker detection, a capture antibody against a specific biomarker protein is first immobilized on a microtiter plate. After the binding of antigen from a sample solution, a labeled detector antibody is allowed to bind with the immobilized antigen. The concentration of the antigen can then be determined by indirectly measuring the concentration of the probe attached to the detector antibody, which include enzymes, fluorescence tags, DNA-barcodes, etc.[1] A typical heterogeneous immunoassay involves antibody immobilization, multiple steps of incubation, and washing cycles, followed by signal amplification and reading. From the initial antibody immobilization to the final reading of the assay results, the entire immunoassay can usually take hours to days to complete. A traditional immunoassay is rather time-consuming and labor-intensive. To overcome these problems, the development of single-step, washing-free homogeneous immunoassays has been of tremendous interest and value to the scientific community.[2]

Gold nanoparticles, including spherical particles, nanorods, and nanoshells with a size ranging from 10s to 100s nanometers, are known to have a large light absorption and scattering cross section in the surface plasmon resonance wavelength regions.[3] The magnitude of light scattering by a gold nanoparticle can be orders of magnitude higher than light emission from strongly fluorescing dyes. This unique property has enabled many important and promising applications of metal nanoparticles in the biomedical field, such as molecular and cell imaging, biosensing, bioassays, and photothermal therapy.[4] However, the strong light scattering property of gold nanoparticles has been mainly applied to optical microscopic imaging of biological cells for qualitative evaluation, but much less frequently for quantitative analysis and assays.

Dynamic light scattering (DLS), also known as photon correlation spectroscopy or quasi-elastic light scattering, is a technique used widely for particle size and size distribution studies. This technique is based on the Brownian motion of spherical particles which causes a Doppler shift of incident laser light. The diffusion constant of particles is measured and the size of the particles is calculated according to the Stokes−Einstein relation.[5] DLS is used routinely to analyze the size and size distribution of polymers, proteins, colloids, and nanoparticles. Because of the strong light scattering property of gold nanoparticles, it is natural to hypothesize that DLS can be a very sensitive technique for quantitative detection and analysis of nanoparticle probes at low concentration.[6] Indeed, it has been demonstrated that DLS can be used to monitor the gold nanoshell concentration in whole blood samples after the intravenous injection of nanoparticles in a murine tumor model[6a] and enzyme to quantum dots interactions.[6b] Although extensive studies have been reported on bioconjugation of gold nanoparticles and biomolecular interaction-directed nanoparticle assembling, to our surprise, DLS has not been used in conjunction with gold nanoparticle probes for homogeneous and quantitative immunoassay. DLS can distinguish individual nanoparticles versus nanoparticle dimers, oligomers or aggregates because of their particle size differences, and this capability makes DLS a potential analytical tool for a quantitative immunoassay.

Prostate specific antigen (PSA), is an FDA-approved biomarker for prostate cancer diagnosis. The total PSA concentration of a healthy male is in the range of a few ng/mL and the free PSA (f-PSA) concentration is typically less than 1 ng/mL, in the range of 10% of the total PSA.[7] Free PSA is the unbound form of prostate specific antigen. Studies have shown that the percentage of f-PSA in total PSA is lower in patients with prostate cancer than those with benign prostate hyperplasia. The free to total PSA ratio is now being introduced and studied as an additional tool for prostate cancer diagnosis. We herein report the development of a highly sensitive one-step homogeneous immunoassay for free PSA detection using gold nanoparticle probes coupled with dynamic light scattering analysis. As illustrated in Scheme 1, two different types of gold nanoparticles (here one is a spherical nanoparticle and one is a nanorod), are to be conjugated with an anti-PSA antibody pair, one with a capture antibody and one with a detector antibody. When these two bioconjugated nanoparticles are mixed in a sample solution that contains antigen f-PSA, the binding of f-PSA will cause nanoparticles to form dimers, oligomers, or aggregates, depending on the concentration of the antigen. Through DLS analysis, the relative ratio of nanoparticle dimers, oligomers, or aggregates versus individual nanoparticles can be measured quantitatively. This ratio should increase accordingly with increased amount of antigen in sample solution, and such a correlation will form the analytical basis of a homogeneous immunoassay.

To demonstrate the feasibility and sensitivity of DLS for immunoassay using gold nanoparticle probes, we first conducted a DLS analysis of nanoparticle materials used in this study. Two types of gold nanoparticles, a citrate-stabilized gold nanoparticle (GNP) and a cetyltrimethyl ammonium bromide (CTAB)-protected gold nanorod (GNR), were synthesized following the literature procedures.[8] The gold nanoparticles have an average core diameter of 37 nm, and the nanorods have a dimension of 10 by 40 nm, as determined from TEM analysis (Figure 1a and b). The actual concentrations of the as-synthesized gold nanoparticles and nanorods were determined by a graphite furnace atomic absorption spectroscopy, combined with UV−vis absorption spectroscopy (Supporting Information). The nanoparticle and nanorod solutions were then diluted to appropriate concentrations for DLS analysis. Figure 1c is the plots of the average scattered light intensity versus nanoparticle and nanorod concentration as measured by DLS. Both

 10.1021/ja711298b CCC: $40.75 © 2008 American Chemical Society

Scheme 1. A Schematic Illustration of a Homogeneous Immunoassay Using Antibody-Conjugated Nanoparticles and Nanorods Coupled with Dynamic Light Scattering Measurement[a]

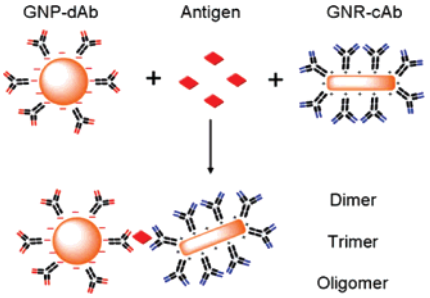

[a] Abbreviations: GNP, citrate-protected gold nanoparticles; dAb, anti-PSA detector antibody; GNR, gold nanorods; cAb, anti-PSA capture antibody.

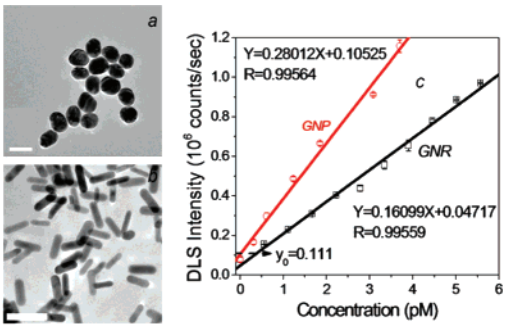

Figure 1. TEM micrographs of (a) gold nanoparticles (scale bar: 50 nm), (b) gold nanorods (scale bar: 60 nm), and (c) their dynamic light scattering intensities and linear regression curves.

gold nanoparticles and nanorods demonstrate a linear increase of scattered light intensity versus concentration in the picomolar range. A detection limit of 0.02 pM (low fM range) for gold nanoparticles and 0.4 pM for gold nanorods was established, which is similar to the reported result of gold nanoshell.[6a] These detection limits are nine orders of magnitudes lower than protein or DNA molecules and four orders of magnitudes lower than sensors based on light absorption.[9] By attaching a metal nanoparticle probe to biomacromolecules such as antibody, it is possible to develop a highly sensitive immunoassay using the DLS technique.

For the immunoassay development, the citrate-protected spherical nanoparticles were conjugated with a detector antibody (GNP-dAb), while the CTAB-protected gold nanorods were conjugated with the capture antibody (GNR-cAb) (Supporting Information).[10] Through our study, it was found that because of the surface positive charge of the CTAB-stabilized gold nanorods, the capture antibody can be conjugated more effectively to nanorods than the citrate-stabilized nanoparticles, while the detector antibody can be conjugated more effectively to the negatively charged citrate-stabilized gold nanoparticles. The successful conjugation of nanoparticles with detector antibody and nanorods with capture antibody was first confirmed by DLS measurement and UV−vis spectral analysis (Supporting Information, Figures S1 and S2). After conjugation with the primary antibodies, the average diameter of gold nanoparticles increased from 37 to 57 nm, while the hydrodynamic dimension of nanorods increased from 30 to 37 nm. The UV−vis spectra revealed a slight shift of the surface plasmon resonance in both intensity and wavelength. For gold nanoparticles, the SPR band shifted from 535 to 541 nm upon antibody conjugation. This shift is most likely caused by the surface chemistry change of the nanoparticles from a citrate-ligand layer to an antibody layer. For the gold nanorods, changes in the SPR band peak wavelengths as well as relative ratio of the two SPR

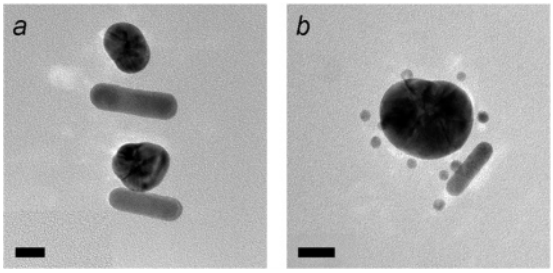

Figure 2. TEM micrographs of (a) nanoparticle-nanorod conjugate oligomers formed from the binding of primary antibody-conjugated gold nanoparticles (GNP-dAb) and gold nanorods (GNR-cAb) nanoprobes with antigen f-PSA (concentration 2 ng/mL); and (b) nanoparticle−nanorod pair after further conjugation with antimouse secondary antibody-conjugated 5 nm gold nanoparticles (scale bar: 20 nm).

bands were observed. The longitudinal SPR band at 733 nm blue-shifted to 725 nm and the transverse SPR band at 516 nm red-shifted to 518 nm. The relative intensity of the longitudinal versus the transverse band decreased from 2.7 to 1.6, corresponding to what has been observed previously from a gold nanorod bioconjugate reported by Rayavarpu et al.[11]

To further confirm the successful conjugation of the two antibodies to the nanoparticles and nanorods, we analyzed the coupling product of the nanoparticle probes with antigen f-PSA in solution using TEM. A 1:2.5 mixture solution of the two nanoprobes, GNP-dAb:GNR-cAb, was added to a buffer solution of f-PSA with a concentration of 2 ng/mL. The mixed solution was incubated for 30 min at 37 °C, and then drop cast on a copper grid and examined by TEM. During the imaging, we observed a large amount of nanoparticle−nanorod dimers as shown in Figure 2a (more TEM micrographs in Figure S3). These nanoparticle dimer and oligomers are believed to be formed through antigen binding with capture antibodies from the nanorods and detector antibodies from the spherical nanoparticles. With increased f-PSA concentration, the amount of such nanoparticle−nanorod pairs and aggregates increased accordingly. To further verify that the nanoparticle−nanorod pairs and oligomers were formed from the binding between antigen f-PSA and the primary antibodies attached to nanoprobes, we added a secondary antimouse IgG-labeled gold nanoparticle (5 nm) into the mixed nanoparticle, nanorods, and f-PSA solution. After incubation for 60 min, the solution was cast on a copper grid and examined by TEM. The TEM micrographs as shown in Figure 2b revealed that most 5 nm gold nanoparticles appeared on the surface or vicinity of large nanoparticles and nanorods, owing to the binding of secondary antibody from the 5 nm nanoparticles to the primary antibodies on the surface of large nanoparticles and nanorods.

The homogeneous immunoassay of f-PSA was then conducted in solution using the conjugated nanoparticles and nanorods coupled with dynamic light scattering measurement. The two nanoprobes were mixed in 1:2.5 (GNP-dAb:GNR-cAb) ratio and then added to the standard f-PSA solutions with different concentrations. After incubating for 30 min, the solutions were diluted to appropriate concentrations for DLS analysis. Figure 3a and b are the size distribution of pure conjugated nanoparticles and nanorods, respectively, while Figure 3c is the size distribution of mixed nanoprobe solution in the presence of 1 ng/mL of f-PSA. For the pure nanoparticle and nanorod conjugates, only one size of particles was observed from the distribution. With f-PSA added to the nanoprobe solution, DLS measurement detected two particle sizes (peak area A and B), one is centered at below 60 nm representing individual nanoparticles and nanorods, and one is above 100 nm corresponding to nanoparticle−nanorod oligomers. The relative ratio of nanopar-

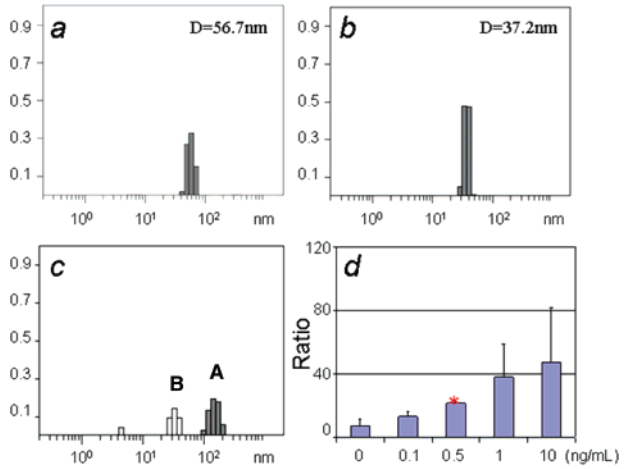

Figure 3. Hydrodynamic diameter distribution plots as determined by DLS measurements: (a) nanoparticle-detector antibody conjugates (GNP-dAb, 5 pM); (b) nanorod-capture antibody conjugates (GNR-cAb, 5 pM); (c) a 1:2.5 mixture of GNP-dAb:GNR-cAb in the presence of f-PSA (1.0 ng/mL); and (d) the calculated numerical ratio of nanoparticle oligomers in the size range of 60−500 nm (peak area A) versus individual particles in the size range of 20−60 nm (peak area B) according to DLS measurement at different f-PSA level (the unknown sample has a concentration of 0.5 ng/mL, data labeled with an asterisk).

ticle oligomers in the size range of 60−500 nm (area A) versus individual nanoparticles in the size range of 20−60 nm range (area B) can be numerically calculated from the size distribution curve. Figure 3d is the plot of this numerical ratio versus f-PSA concentration (DLS data in Supporting Information, Figure S4). With increased concentration of f-PSA, the relative percentage of nanoparticle oligomers increased while the percentage of individual nanoprobes decreased. Using the same nanoprobes in buffer solution, we conducted the analysis of an unknown sample solution (f-PSA concentration at 0.5 ng/mL). The determined concentration corresponds very well to the true concentration of the sample (Figure 3d, data indicated with an asterisk). It is very important to mention here that the standard f-PSA solutions, including the control solution, were actually prepared in a protein matrix solution to simulate the protein content of human serum samples. It was noticeable that when the two nanoprobes were added to the control solution with 0 ng/mL f-PSA, a certain level of nanoparticle oligomer formation was observed, according to DLS analysis. The aggregation is most likely caused by the high content of proteins and high ionic strength of the matrix solution. However, our study demonstrated that even with a small level of nanoparticle instability and aggregation, a quantitative immunoassay is still possible in complex biological fluids using our developed approach. Recently, it was reported by Liu C.-H. et al.[2e] that the light scattering by metal nanoparticles can be detected directly by a fluorescence spectrometer and further used for quantitative DNA detection. In this study, we obtained the average scattered light intensity of each assay solution from DLS measurement; however, we did not find a clear correlation between the average scattered light intensity versus antigen concentration in solution. The comparative ratio of nanoparticle oligomers versus individual particles as determined by DLS measurement appears to provide a more accurate bioassay.

We also conducted a control experiment to demonstrate the selectivity of the assay. The mixed nanoprobe solution was added to solutions that contain a different cancer biomarker, CA125. The oligomer versus individual nanoparticle ratio remained unchanged at different concentrations of CA125 (Supporting Information, Figure S5). This comparison study revealed a good selectivity of the nanoprobe immunoassay.

In summary, we demonstrated here a promising one-step homogeneous immunoassay. By taking advantage of the large scattering cross section of gold nanoparticles and the high sensitivity of DLS measurement, biomarker proteins or other biotargets can be detected at very low concentration using gold nanoparticle probes. As opposed to the traditional plate-based immunoassay, our assay is conducted in solution, which allows a much better mixing and antibody−antigen interaction. The assay does not involve any washing cycle and the assay result can be read as soon as the nanoprobe−sample incubation is completed. Moreover, extremely small amounts of samples are needed for the assay (in this study, about 3.3 μL sample solution was used for each assay). This sample volume can be further decreased by orders of magnitude by using the most advanced DLS technique. We are currently conducting further studies to improve the stability of nanoparticle bioconjugates and optimize the assay conditions to make it suitable for direct analysis of protein biomakers from human serum samples.

Acknowledgment. This work is supported by National Science Foundation CAREER award DMR 0552295 and NIRT award 0506531.

Supporting Information Available: Experimental details, TEM micrographs of nanoparticle−nanorod oligomers. This material is available free of charge via the Internet at http://pubs.acs.org.

References

(1) (a) Yu, F.; Persson, B.; Lofas, S.; Knoll, W. *Anal. Chem.* **2004**, *76*, 6765−6770. (b) Healy, D. A.; Hayes, C. J.; Leonard, P.; McKenna, L.; O'Kennedy, R. *Trends Biotechnol.* **2007**, *25*, 125−131. (c) Das, J.; Aziz, M. A.; Yang, H. *J. Am. Chem. Soc.* **2006**, *128*, 16022−16023.

(2) (a) Warnick, G. R.; Nauck, M.; Rifai, N. *Clin. Chem.* **2001**, *47*, 1579−1596. (b) Weigum, S. E.; Floriano, P. N.; Christodoulides, N.; McDevitt, J. T. *Lab Chip* **2007**, *7*, 995−1003. (c) Kokko, T.; Kokko, L.; Soukka, T.; Lovgren, T. *Anal. Chim. Acta* **2007**, *585*, 120−125. (d) Xu, X.; Georganopoulou, D. G.; Hill, H. D.; Mirkin, C. A. *Anal. Chem.* **2007**, *79*, 6650−6654. (e) Du, B.-A.; Li, Z.-P.; Liu, C-H. *Angew. Chem., Int. Ed.* **2006**, *45*, 8022−8025.

(3) (a) Nikoobakht, B.; El-Sayed, M. *Chem. Mater.* **2003**, *15*, 1957−1962. (b) Link, S.; El-Sayed, M. A. *J. Phys. Chem. B* **1999**, *103*, 8410−8426. (c) Sun, Y.; Xia, Y. *Science* **2002**, *298*, 2176−2179.

(4) (a) Katz, E.; Willner, I. *Angew. Chem., Int. Ed.* **2004**, *43*, 6042−6108. (b) El-sayed, I. H.; Huang, X.; El-Sayed, M. A. *Nano Lett.* **2005**, *5*, 829−834. (c) Huang, X.; El-sayed, I. H.; Qian, W.; El-sayed, M. A. *J. Am. Chem. Soc.* **2006**, *128*, 2115−2120.

(5) Berne, B. J.; Pecora, R. *Dynamic ligh scattering: with applications to chemistry, biology, and physics*; Wiley: New York, 1976.

(6) (a) Xie, H.; Gill-Sharp, L. K.; O'Neal, D. P. *Nanomed.: Nanotechnol., Biol., Med.* **2007**, *3*, 89−94. (b) Ipe, B. I.; Shukla, A.; Lu, H.; Zou, B.; Rehage, H.; Niemeyer, C. M. *ChemPhysChem* **2006**, *7*, 1112−1118.

(7) Sahab, Z. J.; Semaan, S. M.; Sang, Q.-X. A. *Biomarker Insights* **2007**, *2*, 21−43.

(8) (a) Frens, G. *Nat. Phys. Sci.* **1971**, *241*, 20−22. (b) Nikoobakht, B.; El-Sayed, M. A. *Chem. Mater.* **2003**, *15*, 1957−1962.

(9) (a) Pecora, R. *J. Nanopart. Res.* **2000**, *2*, 123−131. (b) Sorlie, S. S.; Pecora, R. *Macromolecules* **1998**, *21*, 1437−1449. (c) Hirsch, L. R.; Jackson, J. B.; Lee. A.; Halas, N. J.; West, J. L. *Anal. Chem.* **2003**, *75*, 2377−2381.

(10) (a) Roe, C. D.; Courtoy, P. J.; Baudhuin, P. *J. Hisochem. Cytochem.* **1987**, *35*, 1191−1198. (b) Brewer, S. H.; Glomm, W. R.; Johnson, M. C.; Knag, M. K.; Franzen, S. *Langmuir* **2005**, *21*, 9303−9307. (c) Ackerson, C. J.; Jadzinsky, P. D.; Jensen, G. J.; Kornberg, R. D. *J. Am. Chem. Soc.* **2006**, *128*, 2635−2640.

(11) Rayavarpu, R. G.; Petersen, W.; Ungureanu, C.; Post, J. N.; Leeuwen, T. G.; Manohar, S. *Int. J. Biomed. Imaging* **2007**, 29817.

JA711298B